Criteria for emittance compensation in high-brightness photoinjectors

Chun-xi Wang* and Kwang-Je Kim
Argonne National Laboratory, 9700 South Cass Avenue, Argonne, Illinois 60439, USA

Massimo Ferrario
INFN-Laboratori Nazionali di Frascati, Via E. Fermi 40, 00044 Frascati, Italy

An Wang†
University of Science and Technology of China, Hefei, China
(Received 2 July 2007; published 3 October 2007)

A critical process in high-brightness photoinjectors is emittance compensation, which brings under control the correlated transverse emittance growth due to the linear space-charge force. Although emittance compensation has been used and studied for almost two decades, the exact criteria to achieve emittance compensation is not as clear as it should be. In this paper, a perturbative analysis of slice envelopes and emittance evolution close to any reference envelope is developed, via which space-charge and chromatic effects are investigated. A new criterion for emittance compensation is found, which is complementary to the well-known matching condition for the invariant envelope and agrees very well with simulations.

DOI: 10.1103/PhysRevSTAB.10.104201 PACS numbers: 29.27.Bd, 41.75.−i, 41.85.−p, 29.25.Bx

I. INTRODUCTION

Under conditions that yield high-quality, well-behaved beams, the transverse dynamics in photoinjectors is dominated by the reduced envelope equation [1],

$$\hat{\sigma}'' + \frac{\kappa}{\beta^2\gamma^2}\hat{\sigma} - \frac{\kappa_s}{\beta^2\gamma^2}\frac{1}{\hat{\sigma}} - \frac{\epsilon_n^2}{\hat{\sigma}^3} = 0. \tag{1}$$

Here we consider axisymmetric systems and use the reduced coordinates $\hat{\sigma} = \sqrt{\beta\gamma}\sigma$, where $\beta\gamma$ is the dimensionless momentum of the reference particle and σ is the rms beam size. κ is the external focusing strength due to solenoid as well as (ponderomotive) rf focusing, κ_s is beam perveance, and ϵ_n is the normalized rms emittance. For a space-charge-dominated beam, the emittance term is much smaller than the space-charge term and thus can be omitted in most cases.

Since the external focusing, and especially the space-charge defocusing, depend on the longitudinal positions, each longitudinal slice follows its own envelope evolution, which may be quite different from the central reference slice. Thanks to the longitudinal laminarity, the envelope equations of all slices are independent of each other and coupled only through the evolution of slice parameters such as the perveance. While the emittance of an individual slice can be considered constant, the total projected emittance

$$\epsilon_{\text{tot}} \equiv \sqrt{\langle\hat{\sigma}^2\rangle\langle\hat{\sigma}'^2\rangle - \langle\hat{\sigma}\hat{\sigma}'\rangle^2} \tag{2}$$

can vary dramatically, where $\langle\cdots\rangle$ indicates averaging over slices. A main task in photoinjector design is to control the projected emittance growth—a process known as emittance compensation [2]. Simulations based on envelope equations of a large number of slices have successfully captured emittance evolution in photoinjectors [3] and compared well with particle-by-particle tracking and experiments [4].

On the theoretical front, the special equilibrium solution (the invariant envelope) [5,6]

$$\hat{\sigma}_{\text{inv}} = \sqrt{\frac{\kappa_s}{\kappa}}, \qquad \hat{\sigma}'_{\text{inv}} = 0 \tag{3}$$

of Eq. (1) was found over a decade ago for a space-charge dominated constant channel, where κ and κ_s are constant and the emittance term can be dropped. Emittance oscillation close to this quasiequilibrium in a booster represents the current model of emittance compensation and Eq. (3) provides matching conditions of practical importance. Nonetheless, this model is inadequate for describing the emittance-compensation process from the cathode to the booster entrance (the original compensation process of Carlsten [2]) because the slices could be far away from equilibrium and furthermore there is no equilibrium at all in the drift space. As a result of this deficiency, the criteria to achieve emittance compensation (especially the condition to minimize the unavoidable mismatches for achieving small emittance) is not as clear as it should be in theory, and simulation is the only option for design in practice.

To overcome this deficiency, we developed a perturbative framework for investigating envelope evolutions close to any reference envelope instead of the special invariant

*wangcx@aps.anl.gov; http://www.aps.anl.gov/~wangcx
†Visiting student of Argonne National Laboratory.

envelope $\bar{\sigma}_{\rm inv}$. Through detailed analysis, we identified the major driving terms for the nearby envelopes and established simple perturbative solutions that can capture the basic dynamics of envelope and emittance evolution from the cathode to the booster and beyond. Assuming the slice dependence of the driving terms dominate and smooth out their s-dependence, an additional criterion for emittance compensation is found, which complements the well-known matching condition in Eq. (3) by providing a condition for minimizing the unavoidable mismatches to the invariant envelope. The new criterion agrees very well with simulations.

To assist our analysis and illustrate the results, we use the optimized design of the SPARC photoinjector [7], which is a typical high-brightness photoinjector. Slice envelopes, as well as other design information, are extracted from HOMDYN [8] simulation, which has been benchmarked with particle-tracking programs [9] such as PARMELA. In this paper, we focus more on the emittance compensation from the cathode to the booster entrance, where invariant envelope theory does not apply.

II. PERTURBATIVE ENVELOPE SOLUTIONS

Using $\bar{\kappa}$, $\bar{\kappa}_s$, and $\bar{\sigma}$ for the reference slice, and using $\Delta\kappa = \kappa - \bar{\kappa}$, $\Delta\kappa_s = \kappa_s - \bar{\kappa}_s$, and $\delta\sigma = \hat{\sigma} - \bar{\sigma}$ for the small derivations of a nearby slice, we can rewrite the envelope equation, Eq. (1), in a form suitable for perturbative treatment as

$$\begin{aligned}
&\hat{\sigma}'' + \frac{1}{\beta^2\gamma^2}\left[\bar{\kappa} + \frac{\bar{\kappa}_s}{\bar{\sigma}^2} + 3\rho\frac{\bar{\kappa}_s}{\bar{\sigma}^2}\right]\hat{\sigma} \\
&= \frac{\bar{\kappa}_s}{\beta^2\gamma^2\bar{\sigma}}\left[\frac{\hat{\sigma}}{\bar{\sigma}} + \frac{\kappa_s}{\bar{\kappa}_s}\frac{\bar{\sigma}}{\hat{\sigma}} - \frac{\Delta\kappa}{\bar{\kappa}_s}\bar{\sigma}\,\hat{\sigma} + \rho\left(\frac{\bar{\sigma}^3}{\hat{\sigma}^3} + 3\frac{\hat{\sigma}}{\bar{\sigma}}\right)\right] \\
&= \frac{\bar{\kappa}_s}{\beta^2\gamma^2\bar{\sigma}}\left[2 + \frac{\Delta\kappa_s}{\bar{\kappa}_s}\frac{\bar{\sigma}}{\hat{\sigma}} - \frac{\Delta\kappa}{\bar{\kappa}_s}\bar{\sigma}\,\hat{\sigma} + \frac{\delta\sigma^2}{\bar{\sigma}\,\hat{\sigma}} + \rho\left(\frac{\bar{\sigma}^3}{\hat{\sigma}^3} + 3\frac{\hat{\sigma}}{\bar{\sigma}}\right)\right] \\
&\simeq \frac{\bar{\kappa}_s}{\beta^2\gamma^2\bar{\sigma}}\left[2 + 4\rho + \frac{\Delta\kappa_s}{\bar{\kappa}_s} - \frac{\Delta\kappa}{\bar{\kappa}_s}\bar{\sigma}^2 + (1+6\rho)\frac{\delta\sigma^2}{\bar{\sigma}^2}\right. \\
&\quad \left. - \frac{\Delta\kappa_s}{\bar{\kappa}_s}\frac{\delta\sigma}{\bar{\sigma}} - \frac{\Delta\kappa}{\bar{\kappa}_s}\bar{\sigma}\delta\sigma + \cdots\right],
\end{aligned} \tag{4}$$

where $\rho \equiv (\beta\gamma\epsilon_n/\sqrt{\bar{\kappa}_s}\bar{\sigma})^2$ is the ratio of the emittance term to the space-charge term in Eq. (1). Note that the coefficient of $\hat{\sigma}$ is the linearized focusing around the reference envelope. We have used, in the second step,

$$\begin{aligned}
\frac{\hat{\sigma}}{\bar{\sigma}} + \frac{\kappa_s}{\bar{\kappa}_s}\frac{\bar{\sigma}}{\hat{\sigma}} &= \frac{\hat{\sigma}}{\bar{\sigma}} + \frac{\bar{\sigma}}{\hat{\sigma}} + \frac{\Delta\kappa_s}{\bar{\kappa}_s}\frac{\bar{\sigma}}{\hat{\sigma}} \\
&= 2 + \frac{\bar{\sigma}}{\hat{\sigma}}\left(1 - \frac{\hat{\sigma}}{\bar{\sigma}}\right)^2 + \frac{\Delta\kappa_s}{\bar{\kappa}_s}\frac{\bar{\sigma}}{\hat{\sigma}},
\end{aligned}$$

and expanded to the second order in small deviations in the last step. The left-hand side of Eq. (4) is the linear focusing part of the envelope equations for all slices in the neighborhood of the reference envelope. The right-hand side is the inhomogeneous as well as nonlinear parts. Given the information of the reference slice, the neighboring slices can be solved perturbatively.

To the linear order in small deviations, we have an inhomogeneous first-order ordinary differential equation (ODE) for the envelope deviations,

$$\begin{bmatrix} \delta\sigma \\ \delta\sigma' \end{bmatrix}' = \begin{bmatrix} 0 & 1 \\ -K(s) & 0 \end{bmatrix}\begin{bmatrix} \delta\sigma \\ \delta\sigma' \end{bmatrix} + F_{\rm sc}\begin{bmatrix} 0 \\ d \end{bmatrix}, \tag{5}$$

where the linear focusing strength

$$K \equiv \frac{1}{\beta^2\gamma^2}\left[\bar{\kappa} + \frac{\bar{\kappa}_s}{\bar{\sigma}^2} + 3\rho\frac{\bar{\kappa}_s}{\bar{\sigma}^2}\right], \tag{6}$$

the space-charge force

$$F_{\rm sc} \equiv \frac{\bar{\kappa}_s}{\beta^2\gamma^2\bar{\sigma}}, \tag{7}$$

and

$$d \equiv \frac{\Delta\kappa_s}{\bar{\kappa}_s} - \frac{\Delta\kappa}{\bar{\kappa}_s}\bar{\sigma}^2 \tag{8}$$

is the perturbations to the inhomogeneous driving term. The general solution of Eq. (5) reads

$$\begin{bmatrix} \delta\sigma \\ \delta\sigma' \end{bmatrix} = R(s)\begin{bmatrix} \delta\sigma_0 \\ \delta\sigma_0' \end{bmatrix} + R(s)\int_0^s d\zeta F_{\rm sc}R^{-1}(\zeta)\begin{bmatrix} 0 \\ d \end{bmatrix}, \tag{9}$$

where $R(s)$ is the transfer matrix from the cathode to location s for the homogeneous solution.

The nonlinear ODE for the reference slice can also be written formally in a form similar to Eq. (9) as

$$\begin{bmatrix} \bar{\sigma} \\ \bar{\sigma}' \end{bmatrix} = R(s)\begin{bmatrix} \bar{\sigma}_0 \\ \bar{\sigma}_0' \end{bmatrix} + \begin{bmatrix} \xi \\ \xi' \end{bmatrix}, \tag{10}$$

where we have introduced

$$\begin{bmatrix} \xi \\ \xi' \end{bmatrix} = \begin{bmatrix} \bar{\sigma} \\ \bar{\sigma}' \end{bmatrix} - R\begin{bmatrix} \bar{\sigma}_0 \\ \bar{\sigma}_0' \end{bmatrix} = R\int_0^s d\zeta F_{\rm sc}R^{-1}\begin{bmatrix} 0 \\ 2+4\rho \end{bmatrix}. \tag{11}$$

Therefore, to the first order in small deviations, the general solutions for the slices in the neighborhood of a given reference slice can be written as

$$\begin{aligned}
\begin{bmatrix} \hat{\sigma} \\ \hat{\sigma}' \end{bmatrix} &= \begin{bmatrix} \xi \\ \xi' \end{bmatrix} + R(s)\begin{bmatrix} \hat{\sigma}_0 \\ \hat{\sigma}_0' \end{bmatrix} \\
&\quad + R(s)\int_0^s d\zeta F_{\rm sc}R^{-1}(\zeta)\begin{bmatrix} 0 \\ d \end{bmatrix}.
\end{aligned} \tag{12}$$

The first term is an "orbit offset" of the reference envelope due to the nonlinear space-charge term in the envelope equation. The second term is the linear propagation of the initial envelopes. The last term is the envelope deviations driven by variations in both external focusing and space-charge defocusing among slices. Since the linear system is

symplectic with $|R| = 1$, the first two terms by themselves preserve the emittance relative to the reference envelope. On the other hand, without proper control, the last term can cause significant emittance growth.

The second-order correction $\delta\sigma_2$ can be worked out by inserting the first-order corrections of Eq. (9) into the second-order driving terms, which gives

$$d_2 = (1 + 6\rho)\frac{\delta\sigma_1^2}{\bar{\sigma}^2} - \frac{\Delta\kappa_s}{\bar{\kappa}_s}\frac{\delta\sigma_1}{\bar{\sigma}} - \frac{\Delta\kappa}{\bar{\kappa}_s}\bar{\sigma}\delta\sigma_1 \tag{13}$$

and the second-order corrections as

$$\begin{bmatrix} \delta\sigma_2 \\ \delta\sigma_2' \end{bmatrix} = R(s)\int_0^s d\zeta F_{\rm sc}R^{-1}(\zeta)\begin{bmatrix} 0 \\ d_2 \end{bmatrix}. \tag{14}$$

III. EMITTANCE CALCULATION FORMULA

To obtain bunch emittance from the envelope solutions above, we have to compute Eq. (2). Although easy to calculate numerically, the emittance expression is very difficult to manipulate analytically in a straightforward manner. Here we derive a useful formula for handling the rms emittance.

Let us start with a general linear expansion,

$$\begin{bmatrix} X \\ P \end{bmatrix} = \sum_\alpha \begin{bmatrix} X_\alpha \\ P_\alpha \end{bmatrix} q_\alpha. \tag{15}$$

Here X and P are some phase-space variables, e.g., $\hat{\sigma}$ and $\hat{\sigma}'$. $X_\alpha(s)$ and $P_\alpha(s)$ are the linear response function of X and P to certain (stochastic) quantity q_α, which may vary and result in a distribution in phase-space. q_α's in general contain small fluctuations in some variables such as initial conditions, parameters, and so on. Let us assume that q_α's fluctuations are uncorrelated, i.e.,

$$\overline{q_\alpha q_\beta} - \bar{q}_\alpha\bar{q}_\beta = \check{q}_\alpha^2\delta_{\alpha\beta}, \tag{16}$$

where the overhead bar indicates phase-space average, $\check{q}_\alpha \equiv \sqrt{\overline{q_\alpha^2} - \bar{q}_\alpha^2}$ is the standard deviation of q_α, and $\delta_{\alpha\beta}$ is the Kronecker delta. Then the emittance can be calculated as

$$\begin{aligned}
\epsilon^2 &= \left|\overline{\begin{bmatrix} X \\ P \end{bmatrix}[X, P]}\right| = \left|\sum_{\alpha,\beta}\begin{bmatrix} X_\alpha \\ P_\alpha \end{bmatrix}[X_\beta, P_\beta]\overline{q_\alpha q_\beta}\right| \\
&= \left|\sum_{\alpha,\beta}\begin{bmatrix} X_\alpha \\ P_\alpha \end{bmatrix}[X_\beta, P_\beta](\bar{q}_\alpha\bar{q}_\beta + \check{q}_\alpha^2\delta_{\alpha\beta})\right| \\
&= \begin{vmatrix} \mathbf{X}\cdot\mathbf{X} & \mathbf{X}\cdot\mathbf{P} \\ \mathbf{X}\cdot\mathbf{P} & \mathbf{P}\cdot\mathbf{P} \end{vmatrix} = \sum_{\alpha<\beta}(\mathbf{X}_\alpha\mathbf{P}_\beta - \mathbf{X}_\beta\mathbf{P}_\alpha)^2 \\
&= \sum_\alpha W_\alpha^2\check{q}_\alpha^2 + \sum_{\alpha<\beta} W_{\alpha\beta}^2\check{q}_\alpha^2\check{q}_\beta^2,
\end{aligned} \tag{17}$$

where $\mathbf{X}$ stands for the vector $(\bar{X}, X_1\check{q}_1, X_2\check{q}_2, \ldots)$, and so does $\mathbf{P}$. A pair of vertical bars stands for the determinant. The W functions are defined as

$$W_\alpha \equiv \begin{vmatrix} \bar{X} & X_\alpha \\ \bar{P} & P_\alpha \end{vmatrix}, \qquad W_{\alpha\beta} \equiv \begin{vmatrix} X_\alpha & X_\beta \\ P_\alpha & P_\beta \end{vmatrix}. \tag{18}$$

In the second-to-last step we have used the *Lagrange's Identity*. With $P = X'$, the function W is the Wronskian of the two functions involved. To verify and appreciate the power of the formula in Eq. (17), one may try to work out a simple case in brute force. This formula improves upon the result used in [10] for explaining emittance oscillation in drift space. It is more involved to take into account the correlations among fluctuating quantities.

IV. EMITTANCE-COMPENSATION CRITERIA

We have seen various driving terms that may cause emittance growth and oscillation. Their effects are difficult to compute analytically. Nonetheless, we estimate it as, via Eq. (11),

$$\begin{aligned}
&R(s)\int_0^s d\zeta F_{\rm sc}R^{-1}(\zeta)\begin{bmatrix} 0 \\ d \end{bmatrix} \\
&= \frac{\bar{d}}{2}\begin{bmatrix} \xi \\ \xi' \end{bmatrix} + R\int_0^s d\zeta F_{\rm sc}R^{-1}\begin{bmatrix} 0 \\ d - (1+2\rho)\bar{d} \end{bmatrix},
\end{aligned} \tag{19}$$

where $\bar{d}$ is the average part of the driving terms and reflects their overall magnitudes. As we shall see later, the driving terms have large amplitude variations among slices in addition to s-dependence. Let us assume that, because of the large variation in driving-term amplitudes from center to edge slices, the first term dominates at least the correlated variations and the second term can be ignored (note that the residual driving-term average to zero for space-charge dominated beam with $\rho = 0$), then the beam envelope of Eq. (12) can be approximated as

$$\begin{aligned}
\begin{bmatrix} \hat{\sigma} \\ \hat{\sigma}' \end{bmatrix} &= \left(1 + \frac{\bar{d}}{2}\right)\begin{bmatrix} \xi \\ \xi' \end{bmatrix} + R(s)\begin{bmatrix} \hat{\sigma}_0 \\ \hat{\sigma}_0' \end{bmatrix} + \cdots \\
&= \left(1 + \frac{\bar{d}}{2}\right)\begin{bmatrix} \xi \\ \xi' \end{bmatrix} + \hat{\sigma}_0\begin{bmatrix} R_{11} \\ R_{21} \end{bmatrix} + \hat{\sigma}_0'\begin{bmatrix} R_{12} \\ R_{22} \end{bmatrix} + \cdots.
\end{aligned} \tag{20}$$

Insert this envelope expansion into the emittance formula and ignore any correlations, and we obtain the bunch emittance as

$$\epsilon_{\rm tot}^2 = \epsilon_0^2 + W_d^2\,{\rm var}\left(\frac{\bar{d}}{2}\right) + W_\sigma^2\,{\rm var}(\hat{\sigma}_0) + W_{\sigma'}^2\,{\rm var}(\hat{\sigma}_0') + \cdots, \tag{21}$$

where

$$\begin{aligned}
W_d \equiv \begin{vmatrix} \bar{\sigma} & \xi \\ \bar{\sigma}' & \xi' \end{vmatrix}, \qquad W_\sigma \equiv \begin{vmatrix} \bar{\sigma} & R_{11} \\ \bar{\sigma}' & R_{21} \end{vmatrix}, \\
W_{\sigma'} \equiv \begin{vmatrix} \bar{\sigma} & R_{12} \\ \bar{\sigma}' & R_{22} \end{vmatrix}
\end{aligned} \tag{22}$$

and ${\rm var}(x)$ stands for the variance of x. In the Wronskians,

the $\bar{\sigma}$ should be the average envelope but its difference from the center reference envelope should be minor. ϵ_0 is from the $\mathrm{var}(\hat{\sigma}_0)\,\mathrm{var}(\hat{\sigma}_0')$ term whose Wronskian is $|R| = 1$. There are two more high-order terms dropped from Eq. (21). One is $(R_{11}\xi' - R_{21}\xi)^2\,\mathrm{var}(\bar{d})\,\mathrm{var}(\hat{\sigma}_0)$, the other is $(R_{12}\xi' - R_{22}\xi)^2\,\mathrm{var}(\bar{d})\,\mathrm{var}(\hat{\sigma}_0')$.

The emittance expression Eq. (21) suggests that, in order to minimize the detrimental effects of various driving terms and accomplish emittance compensation, it is necessary to set

$$W_d = 0 \tag{23}$$

at the location of interest. Particularly, at the entrance of the booster, the beam should be well compensated and matched onto the invariant envelope in the booster with the condition $\bar{\sigma}' = 0$. Therefore, the emittance-compensation criteria at the entrance of the booster s_b can be summarized as

$$W_d(s_\mathrm{b}) = 0 \quad \text{and} \quad \bar{\sigma}'(s_\mathrm{b}) = 0. \tag{24}$$

Let $\bar{\sigma}_R$ represent the linear part of the reference envelope propagated by the matrix R, i.e.,

$$\begin{bmatrix} \bar{\sigma}_R \\ \bar{\sigma}_R' \end{bmatrix} \equiv R(s) \begin{bmatrix} \bar{\sigma}_0 \\ \bar{\sigma}_0' \end{bmatrix}, \tag{25}$$

then, W_d can be rewritten via Eq. (10) as

$$W_d = \begin{vmatrix} \bar{\sigma} & \xi \\ \bar{\sigma}' & \xi' \end{vmatrix} = - \begin{vmatrix} \bar{\sigma} & \bar{\sigma}_R \\ \bar{\sigma}' & \bar{\sigma}_R' \end{vmatrix} = \begin{vmatrix} \bar{\sigma}_R & \xi \\ \bar{\sigma}_R' & \xi' \end{vmatrix}. \tag{26}$$

Thus Eq. (24) implies $\bar{\sigma}'(s_\mathrm{b}) = \bar{\sigma}_R'(s_\mathrm{b}) = \xi'(s_\mathrm{b}) = 0$.

The criteria $\xi'(s_\mathrm{b}) = 0$ can also be viewed as the result of minimizing deviations from the matching condition $\hat{\sigma}' = 0$ for all slices. Since the angle deviations due to various driving terms are given by Eq. (19), a reasonable way to eliminate the effect of such perturbations on $\hat{\sigma}'$ is to get rid of the first term by setting $\xi'(s_\mathrm{b}) = 0$, assuming little could be done for the second term due to uncorrelated/incoherent variations among slices.

The Wronskian in Eq. (26) has an interesting integral expression. Since both $\bar{\sigma}$ and ξ satisfy the same envelope equation of Eq. (4), we have

$$W_d' = \xi\bar{\sigma}'' - \xi''\bar{\sigma} = -(2 + 4\rho)F_\mathrm{sc}\bar{\sigma}_R, \tag{27}$$

where the second derivatives are replaced using the envelope equation. By definition we have the initial conditions $\xi(0) = \xi'(0) = 0$ and thus $W_d(0) = 0$. Therefore,

$$W_d(s) = -\int_0^s d\zeta(2 + 4\rho)F_\mathrm{sc}\bar{\sigma}_R \simeq -2\int_0^s d\zeta F_\mathrm{sc}\bar{\sigma}_R. \tag{28}$$

The second expression holds for a space-charge dominated beam. It shows that emittance compensation requires

$$\int_0^{s_\mathrm{b}} d\zeta F_\mathrm{sc}\bar{\sigma}_R = 0. \tag{29}$$

This indicates that $\bar{\sigma}_R$ must change sign (and sufficiently soon, before the space-charge force drop too much) during the process to achieve emittance compensation. Note that the quantity $\bar{\sigma}_R$, defined in Eq. (25), is not the beam envelope $\bar{\sigma}$ (which is $\bar{\sigma}_R + \xi$ and must be positive) and can be negative.

It is also interesting to note that $F_\mathrm{sc}\bar{\sigma}_R$ represents the work done by the linear space-charge force to displace the envelope by $\bar{\sigma}_R$, the linear part of the envelope evolution. Thus, the criteria might be viewed as: The total work done by the space-charge force (on small virtual displacements proportional to the reference envelope) amounts to zero.

V. SPACE-CHARGE AND CHROMATIC EFFECTS

In this and the following sections, we apply our framework to the optimized SPARC photoinjector design. Figure 1 shows the relativistic factor $\beta\gamma$, the external focusing strength $\bar{\kappa}$, and the perveance $\bar{\kappa}_s$ for the central slice. These quantities are extracted from HOMDYN simulation outputs. In addition, the initial conditions as well as perveance and energy deviations of all slices are extracted from HOMDYN. Using these, the envelope equation can be numerically integrated to obtain $\hat{\sigma}$ and $\hat{\sigma}'$ for all slices, from which rms emittance is computed (these computations were done with MATHEMATICA). Various effects are studied by changing the driving terms in the envelope equation. Our main concern is emittance compensation from the cathode to the booster entrance at about 1.5 m, during which the beam is space-charge dominated with $\rho = 0$.

It is well known that space-charge plays a key role in emittance compensation. The perveance deviations among

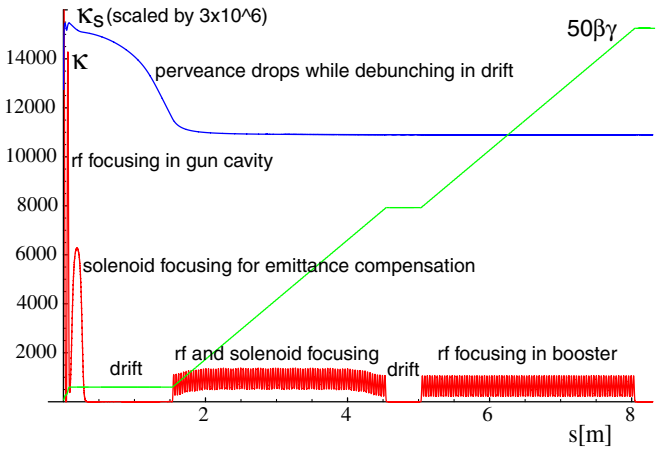

FIG. 1. (Color) $\beta\gamma$, κ [$1/\mathrm{m}^2$], and κ_s of the central slice in green, red, and blue, respectively.

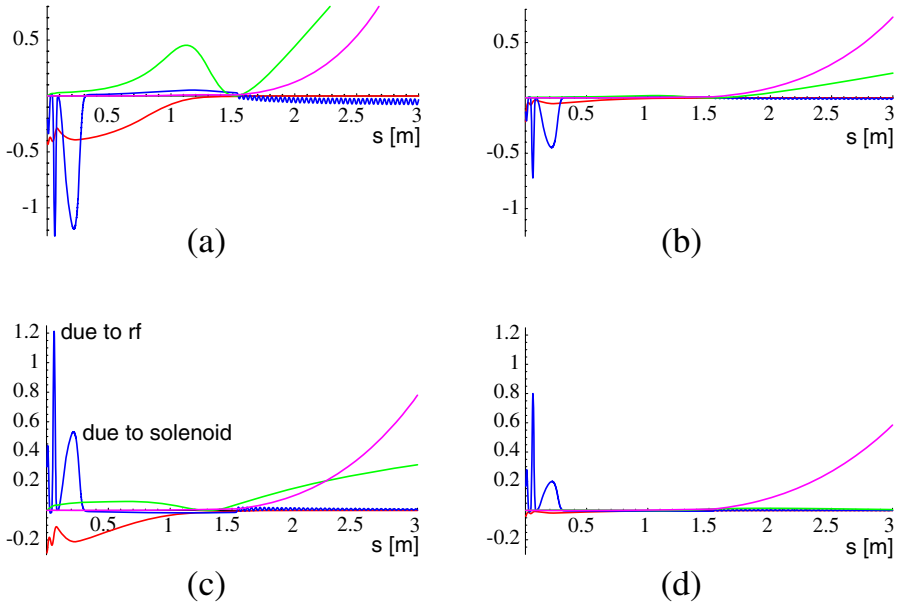

FIG. 2. (Color) Magnitudes of the four dimensionless driving terms in Eq. (4) as a function of s. The curves are, respectively, the space-charge term $\frac{\Delta\kappa_s}{\bar{\kappa}_s}\frac{\bar{\sigma}}{\hat{\sigma}}$ in red, the chromatic term $\frac{\Delta\kappa}{\bar{\kappa}_s}\bar{\sigma}\,\hat{\sigma}$ in blue, and nonlinear terms $\frac{\delta\sigma^2}{\bar{\sigma}\,\hat{\sigma}}$ in green and $\rho(\frac{\bar{\sigma}^3}{\hat{\sigma}^3}+3\frac{\hat{\sigma}}{\bar{\sigma}})$ in magenta. Plots (a) and (b) are for the 3rd and 10th slices from the bunch head. Plots (c) and (d) are for the 3rd and 10th slices from the tail.

slices, $\Delta\kappa_s$ in d of Eq. (8) and (12), yield the slice-dependent space-charge effects. Another key player is the chromatic focusing that varies among slices, arising from the time-dependent rf and solenoid focusing, as suggested in [2,11]. It contributes to the $\Delta\kappa$ in d and is given by the expression [6]

$$\Delta\kappa_c = -\left[\frac{\gamma'^2}{4}+\beta^2\left(\frac{qB_s}{2mc}\right)^2-\beta^2\frac{\bar{\kappa}_s}{\bar{\sigma}^2}\right]\delta_z \simeq -\bar{\kappa}_{\rm tot}\delta_z, \tag{30}$$

where δ_z is the relative deviation of longitudinal kinematic momentum, B_s is the solenoid field strength, and $\bar{\kappa}_{\rm tot}$ is the total focusing strength for the reference slice. The familiar form of chromatic focusing $-\bar{\kappa}_{\rm tot}\delta_z$ applies when $\gamma \gg 1$. In addition to its chromatic effect, the time-dependent rf focusing may contribute a geometric aberration as well (the w_g term in [6]). However, it appears to be small. In the following, we show that space-charge and chromatic effects account for most of the emittance evolution, at least in the case of the SPARC photoinjector.

To examine the magnitudes of the last four driving terms in the square bracket of Eq. (4) before the last-step approximation, we computed each driving term and plotted them in Fig. 2 for the 3rd and 10th slices in the head and in the tail of a 55-slice bunch, respectively. The space-charge and chromatic driving terms are large before the booster entrance, and quite small afterwards. On the other hand, the nonlinear driving terms become large in the booster. These driving terms become quite large (compared to the constant 2) for slices in the head and tail of a bunch. Note that for both space-charge and chromatic driving terms, despite large variations in amplitudes, the shapes are similar among slices. In fact, to a fair approximation, it is

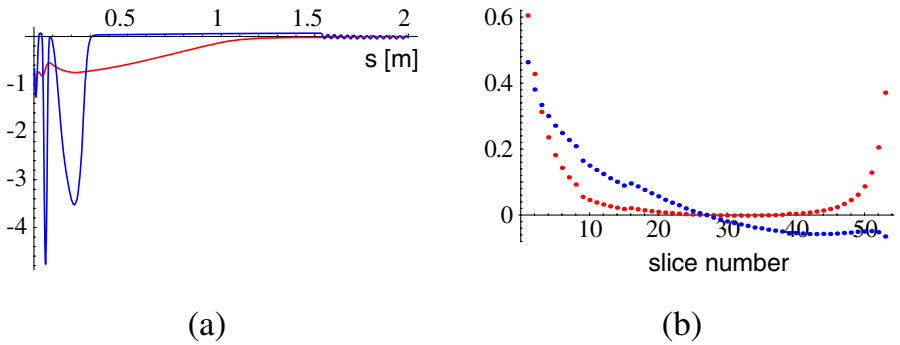

FIG. 3. (Color) Decomposition of space-charge (red) and chromatic (blue) driving terms $\frac{\Delta\kappa_s}{\bar{\kappa}_s}\frac{\bar{\sigma}}{\hat{\sigma}}$ and $\frac{\Delta\kappa}{\bar{\kappa}_s}\bar{\sigma}\,\hat{\sigma}$ into (a) common s-dependent variation and (b) slice-dependent normalized amplitudes.

possible to decompose the driving term in the form $u * f(s)$, where u is a slice-dependent amplitude and f is a s-dependent function common to all slices. Such a decomposition can significantly simplify the computation of the integrals in the envelope solution by taking the slice dependence of driving terms out of the integral. Figure 3 shows the u and f for space-charge as well as chromatic driving terms for the 53 slices used in our computation. (The first and last slices were excluded to avoid potential complications due to discontinuity associated with the beer-can bunch model.) Note that the space-charge term is always negative while the chromatic term changes signs from head to tail.

To examine the effects of these driving terms on the emittance, we numerically solved the envelope equations Eq. (4) for all slices, using the original κ and κ_s of each slice, including only selected driving terms. The results are shown in Fig. 4, which contains six emittance curves: the black one is the HOMDYN result; the other five include from none to all of the four terms shown in Fig. 2. Clearly, the space-charge and chromatic effects account for most of the emittance evolution. The residual difference from HOMDYN could be due to unaccounted effects in our current analysis, such as image charge from the cathode as well as other nonlinear effects.

The first-order space-charge and chromatic effects can be calculated with the simple expression in Eq. (12), which is the solution of Eq. (4) up to first-order perturbations. To examine the validity of this approximate solution, we numerically computed the envelope for each slice with its $\Delta\kappa_s$ and $\Delta\kappa_c$ extracted from the HOMDYN output. The results are plotted in Fig. 5. Again, we see that both space-charge and chromatic effects are significant and together they account for most of the emittance oscillation. It is encouraging to see that first-order perturbation theory works fairly well. The difference between the green and

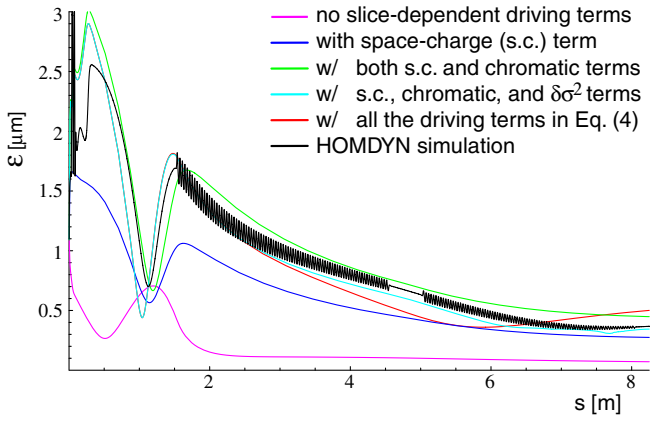

FIG. 4. (Color) Effects of various driving terms on the emittance. The black curve is from HOMDYN. The magenta, blue, green, cyan, and red curves include, respectively, from 0 increasingly up to all 4 driving terms in Eq. (4) in the order that they appear in the equation.

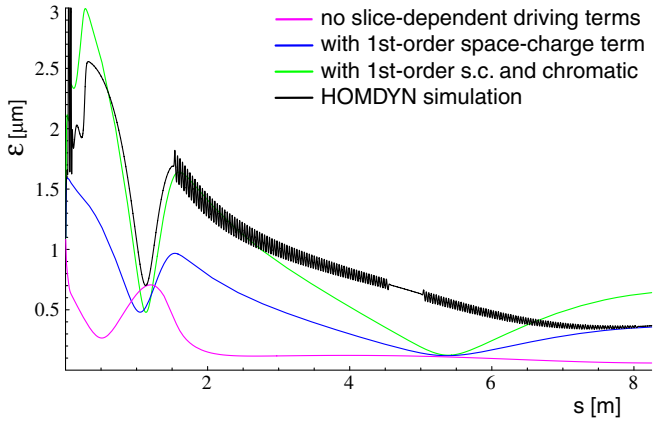

FIG. 5. (Color) Effects of first-order driving terms on the emittance via Eq. (12). The black and magenta curves are the same as in Fig. 4. The blue curve includes only space-charge and the green curve includes both space-charge and chromatic driving terms in Eq. (8).

black curves increases in the boosters because the nonlinear driving terms in Eq. (12) become large with increasing ρ and envelope derivation $\delta\sigma$. It appears that the emittance oscillation is more coherent in these first-order results than the results containing higher-order/nonlinear terms as shown in the previous figure. In other words, nonlinearity suppresses the coherent emittance oscillation and tends to spoil associated emittance compensation. In fact, the emittance minimum close to the entrance of the second booster is apparently wiped out. The green curve ends up above the black one because it is going through a maximum in emittance oscillation.

VI. EMITTANCE COMPENSATION IN SPARC PHOTOINJECTOR

To examine the new criteria for emittance compensation with HOMDYN simulation, Fig. 6 plots the three quantities $\bar{\sigma}'$, $\bar{\sigma}'_R$, and $\bar{\xi}'$ along the injector axis. Clearly they go

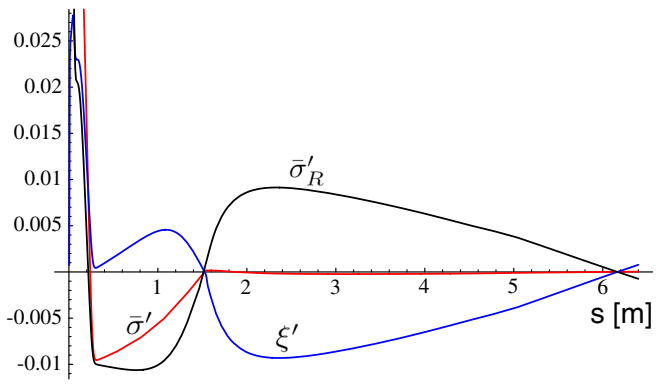

FIG. 6. (Color) $\bar{\sigma}'(s)$ in red, $\bar{\sigma}'_R(s)$ in black, and $\bar{\xi}'(s)$ in blue. Emittance compensation requires $\bar{\sigma}' = \bar{\sigma}'_R = \bar{\xi}' = 0$ at the booster entrance at about 1.5 m.

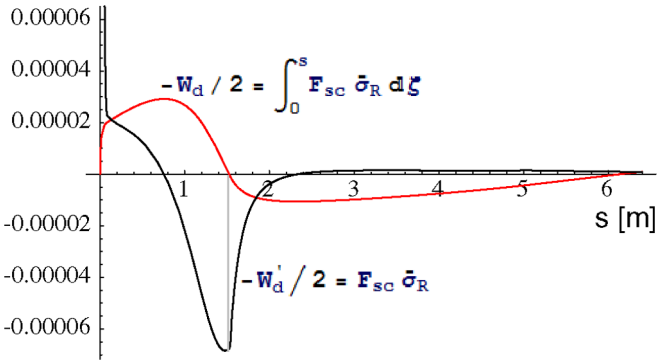

FIG. 7. (Color) $W_d(s)$ in red and $W_d'(s)$ in black. Emittance compensation requires $W_d = 0$ at the booster entrance around 1.5 m.

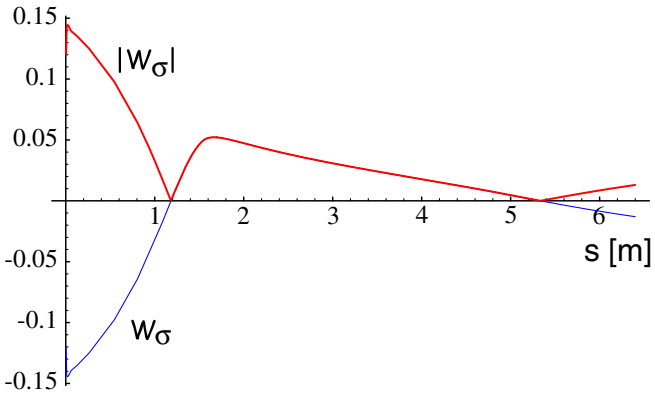

FIG. 8. (Color) W_σ and $|W_\sigma|$ of Eq. (21). Note that the two minimum locations agree with those in Fig. 5.

through zero together at the booster entrance as required for emittance compensation. Note that the optimized HOMDYN simulation was done before the starting of this work, following the criteria of Eq. (3) and scanning in parameter space for minimum emittance. Thus, this is an independent check and strong support of our finding. Emittance compensation also shows up further down the beam line as expected. The Wronskian $W_d(s)$ and its derivative are shown in Fig. 7. Again we see that $W_d = 0$ at the booster entrance as demanded by the emittance-compensation criteria. The area above the axis and under the black W_d' curve is compensated by the area below the axis up until the booster entrance. Note that most of the growth in W_d occurs very close to the cathode when the electrons are still nonrelativistic.

The criteria we obtained agree very well with simulations. In fact, it holds better than we would expect from perturbative treatment and the approximations lead to Eq. (21), which makes us wonder if there might be other explanations. It would be interesting to see if such criteria hold for other optimized photoinjectors, especially those resulting from automated multiobjective optimization [12]. We must mention that, although the $W_d^2\,\mathrm{var}(\bar{d})$ term in Eq. (21) may have captured the essence of correlated contribution to the emittance and thus leads to the emittance-compensation criteria as was demonstrated in Figs. 6 and 7, it may not be suitable for calculating the total emittance in details, for which information presented in Fig. 3 can be used to compute slice envelopes, and correlations need to be considered in emittance computation. It turns out that, after emittance compensation, the W_σ term shown in Fig. 8 dominates the emittance oscillation (especially the two minima) shown in Fig. 5.

ACKNOWLEDGMENTS

This work was supported by U.S. Department of Energy, Office of Science, Office of Basic Energy Sciences, under Contract No. DE-AC02-06CH11357.

[1] See, for example, J. D. Lawson, *The Physics of Charged Particle Beams* (Oxford University Press, New York, 1988), 2nd ed.
[2] B. E. Carlsten, Nucl. Instrum. Methods Phys. Res., Sect. A **285**, 313 (1989).
[3] M. Ferrario, J. E. Clendenin, D. T. Palmer, J. B. Rosenzweig, and L. Serafini, SLAC-PUB-8400, 2000.
[4] See, for example, C. Ronsivalle *et al.*, Proceedings of the 2007 Particle Accelerator Conference (PAC07), 2007, p. 986.
[5] L. Serafini and J. B. Rosenzweig, Phys. Rev. E **55**, 7565 (1997).
[6] C.-x. Wang, Phys. Rev. E **74**, 046502 (2006).
[7] D. Alesini *et al.*, Proceedings of the 9th European Particle Accelerator Conference (EPAC'04), 2004, p. 399.
[8] M. Ferrario and L. Serafini, Proceedings of the 6th European Particle Accelerator Conference (EPAC'98), 1999, p. 1271.
[9] C. Limborg *et al.*, Proceedings of the 2003 Particle Accelerator Conference (PAC'03), 2003, p. 3548.
[10] C.-x. Wang, in Proceedings of the 35th Advanced ICFA Beam Dynamics Workshop on Physics and Application of High Brightness Electron Beams, 2005.
[11] M. Ferrario *et al.*, SPARC-BD-03/003.
[12] I. V. Bazarov and C. K. Sinclair, Phys. Rev. ST Accel. Beams **8**, 034202 (2005).